**PAPER**

Check for updates

# Low-temperature dissociation of CO$_2$ molecules on vicinal Cu surfaces†

Takanori Koitaya, [iD] *[a] Yuichiro Shiozawa,[b] Yuki Yoshikura,[b] Kozo Mukai,[b] Shinya Yoshimoto[b] and Jun Yoshinobu [iD] *[b]

The reaction of carbon dioxide on the vicinal Cu surfaces at low temperatures was investigated by infrared reflection absorption spectroscopy, scanning tunneling microscopy, X-ray photoelectron spectroscopy, and quadrupole mass spectrometry. Dissociation of CO$_2$ molecules into CO on the Cu(997) and Cu(977) surfaces was observed at temperatures between 80 K and 90 K, whereas it did not occur on Cu(111) under a similar condition. CO and physisorbed CO$_2$ were the main adsorbates during the reaction. In contrast, the amount of atomic oxygen on the surface was small. The dissociation of CO$_2$ was promoted by the small amount of oxygen produced by the CO$_2$ dissociation on the Cu surfaces. This leads to the induction period in the CO$_2$ reaction; the initial reaction rate on the clean Cu surfaces was low, and the coadsorbed oxygen enhanced the dissociation reactivity of CO$_2$. Mass analysis of desorption species during the reaction revealed that the observed CO formation on the vicinal Cu surface is mainly caused by an oxygen-exchange reaction with residual CO in an ultra-high vacuum chamber.

## Introduction

Catalytic transformation of carbon dioxide is a challenging topic in C1 chemistry.[1,2] The interaction of CO$_2$ with the catalytic surfaces is essential for the activation of CO$_2$ molecules due to its chemical inertness. Thus, the adsorption and reaction of CO$_2$ on metal and metal-oxide surfaces have been intensively studied to reveal the nature of the interaction between adsorbed CO$_2$ and solid surfaces.[3–6]

CO$_2$ adsorption on the metallic copper surfaces is an important topic for methanol synthesis from CO$_2$ and H$_2$ on Cu/ZnO catalysts.[7] The flat single-crystal Cu surfaces are less reactive for the CO$_2$ reaction. Under an ultrahigh-vacuum (UHV) condition, only physisorbed molecules are observed at temperatures below 80 K.[3,8–10] In contrast to the flat surfaces, higher reactivity of vicinal or polycrystalline Cu surfaces for CO$_2$ has been reported experimentally. The chemisorbed (bent) CO$_2$ molecules were observed by XPS on the polycrystalline Cu,[11] and dissociation into CO was detected by temperature-programmed desorption (TPD) on Cu(332)[12] and Cu(311)[13] surfaces at temperatures between 95 and 200 K. However, there is a report that adsorbed CO$_2$ molecules on the Cu(211) surface do not react and

completely desorb after heating the sample to 120 K.[14] The van der Waals density functional (vdW DF) calculations have shown that the activation energy for CO$_2$ dissociation on vicinal Cu surfaces is larger than 0.67 eV.[15] This theoretical result would suggest that the dissociation hardly occurs on the clean Cu surfaces at low temperatures, especially below 100 K. To untangle the controversial results on the CO$_2$ reactivity on vicinal Cu surfaces, further investigations are required to reveal whether CO$_2$ molecules can dissociate on the Cu surfaces and which factor is important to the CO$_2$ reaction on the low-temperature Cu surfaces. In this study, we investigated the reaction of CO$_2$ on the Cu(111), Cu(997), and Cu(977) surfaces at low temperatures using infrared reflection absorption spectroscopy (IRAS), X-ray photoelectron spectroscopy (XPS), *in situ* quadrupole mass spectroscopy (QMS), and scanning tunneling microscopy (STM).

The CO$_2$ dissociation into CO on the vicinal Cu surfaces at 83 K was detected by IRAS and STM. XPS measurements of the reaction show characteristic uptake curves of the CO produced on the surface; the dissociation rate is increased as a function of elapsed time until reaching near-saturation coverage of CO. The XPS and QMS experiments indicate that the CO$_2$ dissociation observed in this study leads to an oxygen-exchange reaction between CO$_2$ and CO.

*[a] Department of Chemistry, Graduate School of Science, Kyoto University, Kitashirakawa-Oiwakecho, Sakyo-Ku, Kyoto 606-8502, Japan. E-mail: koitaya.takanori.5j@kyoto-u.ac.jp*

*[b] The Institute for Solid State Physics, The University of Tokyo, 5-1-5, Kashiwanoha, Kashiwa, Chiba, 277-8581, Japan. E-mail: junyoshi@issp.u-tokyo.ac.jp*

† Electronic supplementary information (ESI) available. See DOI: https://doi.org/10.1039/d3cp06336d

## Experimental

All experiments were performed under UHV conditions. The Cu(111), Cu(997), and Cu(977) samples (10 mm diameter disk)

**9226** | *Phys. Chem. Chem. Phys.*, 2024, **26**, 9226–9233

This journal is © the Owner Societies 2024

were purchased from the surface preparation laboratory. Cu(997) consists of nine-atom wide (111) terraces separated by monoatomic (111) steps and thus can be labelled as $9(111) \times (111)$ using a microfacet notation. On the other hand, the Cu(977) surface is referred to as $8(111) \times (100)$. The terrace widths of Cu(997) and Cu(977) are 18.7 Å and 17.0 Å, respectively. Before each experiment, these Cu surfaces were cleaned by several cycles of $Ne^+$ ion sputtering and annealing in the 673–700 K range. The temperature of the sample was measured using a K-type thermocouple attached to the side of the Cu crystal by a Ta foil. The samples were cooled by liquid nitrogen.

IRAS measurements were performed in a UHV chamber with a base pressure of $1.3 \times 10^{-8}$ Pa. IRAS spectra were measured using an FT-IR spectrometer (Bruker IFS66v/S) with a mercury–cadmium–telluride (MCT) detector. All the spectra were obtained with 4 $cm^{-1}$ resolution. To investigate the thermal reaction of inert $CO_2$ on the Cu surfaces, it is essential to pay careful attention to the possibility of experimental artifacts.[6] A high-purity isotopic $^{13}CO_2$ gas ($>$99.999% purity) was used for IRAS experiments to differentiate reaction products from the background adsorption of residual $^{12}CO$ in the UHV chamber. During a series of IR measurements, all the filaments, including a hot-cathode vacuum gauge in the chamber, were turned off to exclude the possibilities of the $CO_2$ reaction at a hot filament and electron-induced reactions on the Cu surface. In the IRAS experiments, $CO_2$ gas was introduced into the UHV chamber through a pulse gas dosing system. The gas was first filled in a gas line at a constant pressure of 133 Pa. The gas line is connected to the UHV chamber via a pulse valve (Parker Hannifin Pulse Valves Series 99). $CO_2$ molecules were dosed onto the sample by opening the pulse valve for a certain period (5 ms). The exposure of gaseous molecules was controlled by the number of pulses. The exposure per one pulse shot has been estimated to be 0.065 L from an uptake curve of cyclohexane on Rh(111) [1 L = $1 \times 10^{-6}$ Torr s = $1.33 \times 10^{-4}$ Pa s].[16]

The synchrotron-radiation XPS (SR-XPS) measurements were performed using a UHV chamber (base pressure = $1 \times 10^{-8}$ Pa) at a soft X-ray undulator beamline (BL-13B) of Photon Factory in Tsukuba, Japan. All XPS spectra in this paper were obtained at a sample temperature of 85 K using a hemispherical electron analyzer (SPECS, Phoibos 100) at a normal emission angle with a photon energy of 630 eV. The total instrumental energy resolution was 0.2 eV. The $CO_2$ and CO coverages in the SR-XPS experiments were estimated from C 1s area intensity, which is calibrated by the intensity of a $(1.4 \times 1.4)$ CO superstructure ($\theta_{CO}$ = 0.52 ML; ML = molecules per one surface Cu atom) on Cu(997).[17]

The laboratory XPS measurements with an Al Kα X-ray source ($h\nu$ = 1486.6 eV) were performed in a UHV chamber equipped with a QMS (Balzers, Prisma QME200) and a hemispherical electron analyzer (Scienta Omicron, R3000). The QMS measurements of desorbed species during the surface reaction were also conducted using this chamber. The isotope molecules, $C^{18}O_2$ ($^{18}O$ purity: 94 atom%), were used in the QMS experiments to detect oxygen-containing reaction products from the $CO_2$ dissociation.

The STM experiments of the Cu(997) surface were conducted in another UHV chamber with a low-energy electron diffraction (LEED) apparatus, QMS, and STM (Createc). The density of kink sites of the clean Cu(997) surface was estimated to be less than 0.5% from the STM images of the bare Cu(997) surface. $CO_2$ was dosed on the Cu(997) surface at 80 K and 92 K, followed by post-reaction STM experiments at sample temperatures between 77 K and 80 K. The STM images were obtained using an electrochemically polished tungsten tip.

## Results and discussion

Fig. 1(a) shows a series of IRAS spectra on Cu(997) at 83 K as a function of $^{13}CO_2$ exposure. At exposure below 7 L, two peaks were observed at 2050 and 2067 $cm^{-1}$, assigned to $^{13}CO$ stretching vibrations on the atop site. These peaks were observed at higher wavenumbers than those on the flat Cu(111) surfaces (2031 $cm^{-1}$).[18] The STM experiments shown later (Fig. 2) indicate that the CO molecules produced at low coverage preferentially adsorb on the kink sites, followed by adsorption at the step sites. Therefore, the peak at 2067 $cm^{-1}$, which is more intense at 2 L, is assigned to the $^{13}CO$ at the kink, and the peak at 2050 $cm^{-1}$ can be attributed to the isolated molecules at step sites. At an exposure of 20 L, a new peak of $^{13}CO$ appeared at 2046 $cm^{-1}$, and this peak was shifted to a lower
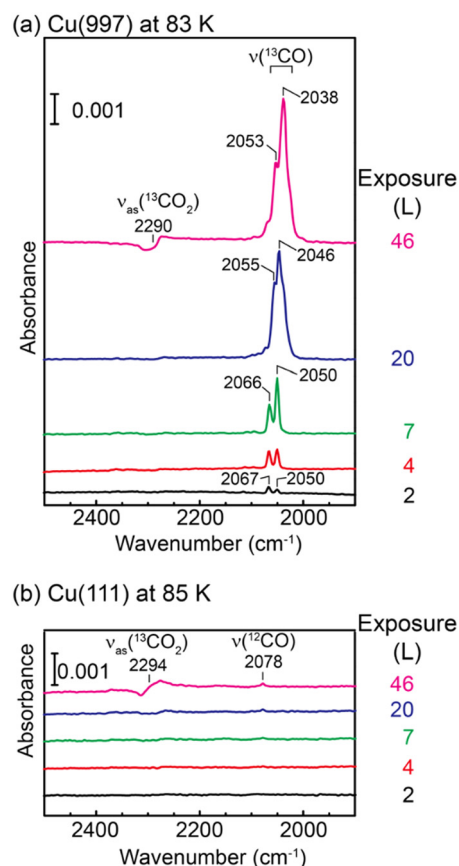


Fig. 1 A series of IRAS spectra of (a) Cu(997) at 83 K and (b) Cu(111) at 85 K as a function of $^{13}CO_2$ exposure.

This journal is © the Owner Societies 2024

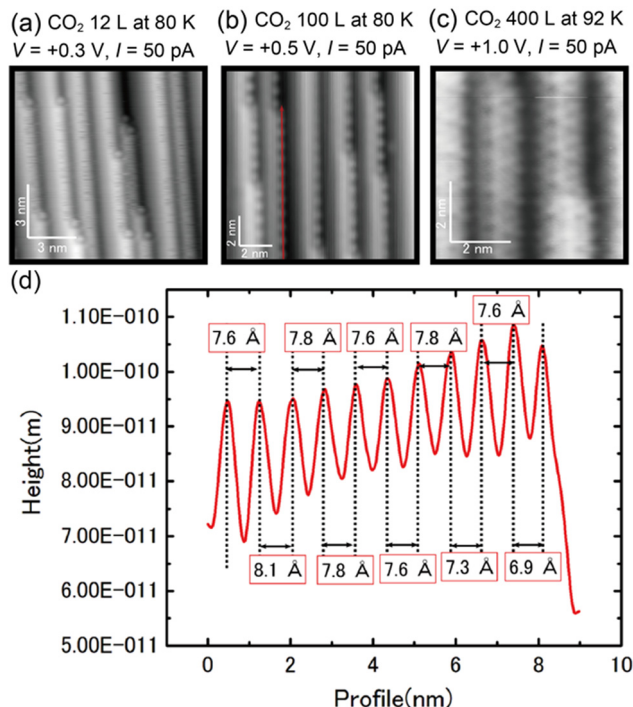*Phys. Chem. Chem. Phys.*, 2024, **26**, 9226–9233 | **9227**

**Fig. 2** (a)–(c) STM images of the Cu(997) surface as a function of $CO_2$ exposure. (d) Line profile along the red arrow in (b).

wavenumber with increasing exposure (2038 cm$^{-1}$ at 46 L). Judging from the STM images (Fig. 2), the coverage of $^{13}CO$ was still low at this exposure, and thus, we attributed this peak to step $^{13}CO$ species at higher coverage. At the exposure of 46 L, the antisymmetric stretching mode of physisorbed $^{13}CO_2$ was observed at 2290 cm$^{-1}$. The asymmetric Fano-like line shape indicates the coupling between the molecular vibrational motion and electronic states of the Cu substrate.[17]

In contrast, IRAS spectra of Cu(111) at 85 K (Fig. 1(b)) show no vibrational mode of adsorbed $^{13}CO$. The main peak at 46 L is assigned to the Fano-like $^{13}CO_2$ antisymmetric stretching mode, and a small peak at 2078 cm$^{-1}$ is assigned to $^{12}CO$.[19] The observation of the $^{12}CO$ molecules is due to the adsorption of background residual $^{12}CO$ gas in the UHV chamber.

The IRAS spectra shown in Fig. 1 are clear evidence of dissociation of $CO_2$ on the vicinal Cu(997) surface at 83 K. Using isotope $^{13}CO_2$ molecules, the possibility of the adsorption of residual $^{12}CO$ molecules in the UHV chamber is ruled out. In addition, the control experiments on the Cu(111) surface exclude the possibility of experimental artifacts such as the adsorption of $^{13}CO$ impurity in the $^{13}CO_2$ gas and electron-stimulated dissociation of $CO_2$, which was suggested by XPS of $CO_2$ on Cu surfaces.[14,20] Therefore, $CO_2$ molecules are dissociated on the Cu(997) surface at 83 K. The low-temperature dissociation indicates a low activation energy for this reaction.

The surface adsorbates by the $CO_2$ exposure were further investigated by STM. Fig. 2(a) shows an STM image of Cu(997) after 12 L $CO_2$ exposure at 80 K. Several protrusions were observed at kink sites after the $CO_2$ exposure. Based on the IRAS results in Fig. 1(a), the protrusions are assigned to CO

adsorbed at the kink sites. Note that the percentage of kink sites was estimated to be less than 0.5% on the Cu(997) clean surface. The CO molecules preferentially adsorbed at kink sites on the Cu(997) surface. In addition, line-noise-like features were often observed at step sites, which were not observed on the clean Cu(997) and the terrace sites on the $CO_2$-exposed Cu(997). Thus, this is probably due to the diffusion of CO molecules along the step. At higher exposure (100 L), the ordered protrusions are observed along the steps (Fig. 2(b)). The line profile along the step (red arrow in Fig. 2(b)) is shown in Fig. 2(d). The average distance between neighboring protrusions was estimated to be 7.7 Å, which is three times longer than the nearest-neighbor distance between surface Cu atoms of the Cu(997) surface (2.56 Å). The obtained images after $CO_2$ exposure are similar to the STM images of the Cu(997) surface after CO exposure (see the ESI,† Fig. S1). This also supports the assignment that the observed protrusions are attributed to the CO molecules. The observed peak wavenumbers in IRAS indicate that CO molecules are adsorbed on the atop site. Therefore, the step CO molecules at the atop sites form a one-dimensional (1 × 3) superstructure. Further exposure of $CO_2$ (400 L) leads to the observation of depressions on the terrace sites. The difference in the images at lower exposures and higher exposure is due to the difference in the state of the tip apex. According to the previous STM study on CO adsorbed on Cu(111), a CO molecule is imaged as a protrusion (depression) with a CO-adsorbed tip (a bare metal tip), respectively.[21] Therefore, the produced CO molecules could also occupy the terrace sites. The present STM result indicates that CO, which is produced at active sites, can diffuse to the terrace and does not suppress further the dissociation reaction of $CO_2$. Significant surface reconstruction was not observed after the $CO_2$ reaction. However, fuzzy protrusions at kink sites were often observed after the $CO_2$ exposure (see the ESI,† Fig. S2). This structure could be attributed to oxygen adsorption at the Cu kink sites, where the atomic oxygen was produced by the $CO_2$ dissociation.

Quantitative analysis of the $CO_2$ dissociation was carried out by SR-XPS. Fig. 3(a) and (b) show a series of XPS C 1s and O 1s spectra of Cu(997) as a function of elapsed time measured under a constant $CO_2$ pressure ($P_{CO_2}$ = 1.8 × 10$^{-6}$ Pa). During the measurements, the sample temperature was maintained at 85 K. A peak at 284.3 eV in the C 1s spectra is attributed to a small amount of atomic carbon contamination (0.02 ML) of the Cu sample. Under the constant $CO_2$ pressure, a peak at 291.4 eV appeared at the exposure time of 60 s, which is assigned to physisorbed $CO_2$. This peak gradually increased in intensity with the increase in reaction time. The peak of physisorbed $CO_2$ disappeared when the chamber was evacuated, indicating that $CO_2$ molecules are in an adsorption–desorption equilibrium at 85 K. At $t$ > 2000 s, new peaks appeared at 286.1 eV with broader peaks at higher binding energies. These peaks are attributed to the main peak and the shake-up satellites of adsorbed CO on Cu.[22] In fact, the positions of the main and satellite peaks are the same as the reference spectrum of CO on Cu(997) at a saturation coverage (0.52 ML). The observation of
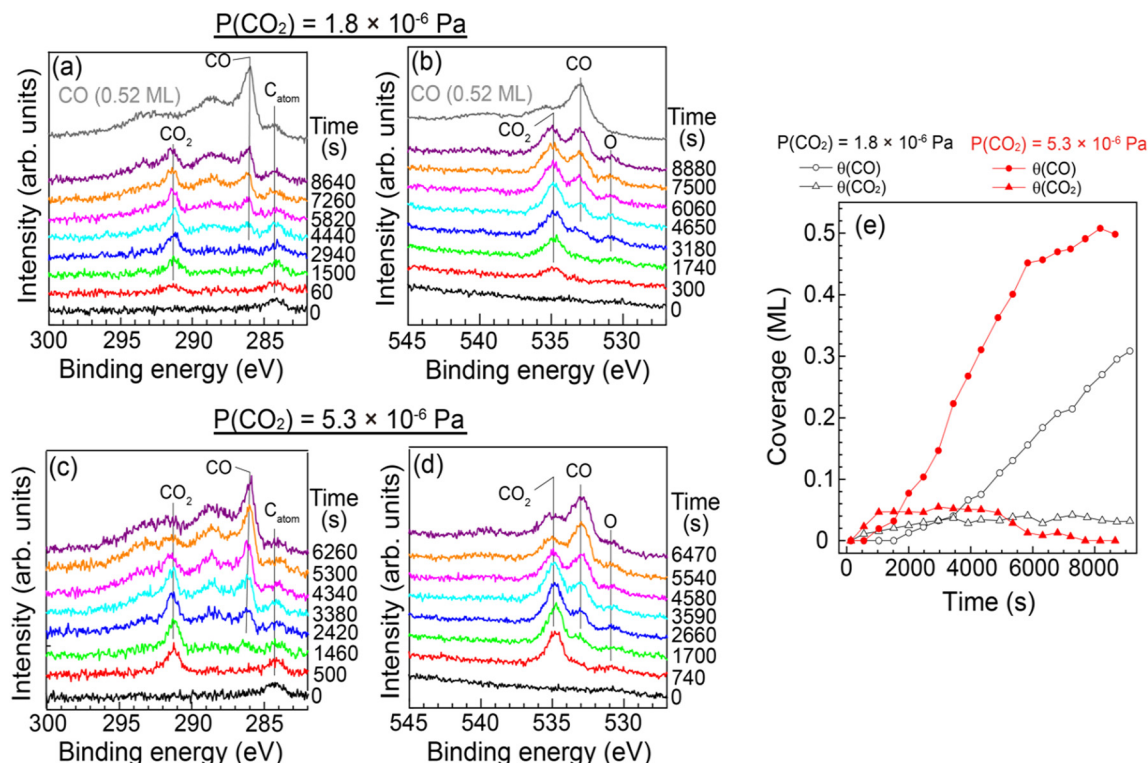
**9228** | *Phys. Chem. Chem. Phys.*, 2024, **26**, 9226–9233

This journal is © the Owner Societies 2024

Fig. 3 (a) C 1s and (b) O 1s SR-XPS spectra on Cu(997) at 85 K as a function of $CO_2$ exposure time together with the reference spectra of adsorbed CO on Cu(997) at saturation coverage (topmost). During the measurement, $CO_2$ pressure was maintained at $1.8 \times 10^{-6}$ Pa. (c) C 1s and (d) O 1s SR-XPS spectra on Cu(997) at 85 K at a $CO_2$ pressure of $5.3 \times 10^{-6}$ Pa. (e) Coverages of adsorbed CO (circles) and $CO_2$ (triangles) estimated from C 1s area intensity at $1.8 \times 10^{-6}$ Pa (open symbols) and $5.3 \times 10^{-6}$ Pa (filled symbols).

CO is consistent with the IRAS and STM measurements. The O 1s spectra in Fig. 3(b) also show the adsorption of $CO_2$ and the formation of CO. In addition, a peak at 530.8 eV was observed as time elapsed, indicating that there is an oxygen-containing coadsorbed species other than $CO_2$ and CO. As discussed later, this peak can be attributed to atomic oxygen coadsorbed with CO and $CO_2$. It should be noted that the peak intensity of atomic oxygen was significantly smaller than that of the CO peaks; coverages of atomic oxygen estimated from O 1s spectra in Fig. 3(b) were less than 0.03 ML. This result indicates that oxygen atoms do not remain on the surface after the $CO_2$ dissociation or migrate into subsurface/bulk sites. Similar experiments were conducted at higher pressure ($5.3 \times 10^{-6}$ Pa). A series of SR-XPS spectra is shown in Fig. 3(c) and (d). The surface reaction process was the same as that at lower pressure; first, the physisorption of $CO_2$ occurred, followed by a gradual increase of surface CO coverage.

The CO and $CO_2$ coverages during the dissociation reaction were estimated from C 1s area intensities (Fig. 3(e)). The $CO_2$ coverage was gradually increased from 0.015 ML at 60 s to 0.04 ML at $t > 3000$ s at $P_{CO_2} = 1.8 \times 10^{-6}$ Pa. As mentioned above, $CO_2$ is in the adsorption–desorption equilibrium at 85 K. Thus, the increase of the $CO_2$ coverage indicates the formation of additional adsorption sites with slightly higher adsorption energy for $CO_2$ than the clean Cu(997) surface. On the other hand, the adsorbed CO molecules appeared at $t \sim 2000$ s, and

the CO coverage increased linearly at $t > 4000$ s. The observed result indicates an induction period before acceleration to the $CO_2$ dissociation. At higher $CO_2$ pressure ($5.3 \times 10^{-6}$ Pa), the equilibrium $CO_2$ coverage was slightly increased (0.05 ML) compared with the lower pressure. The CO formation is faster than that at the lower $CO_2$ pressure, and the CO coverage increased to 0.5 ML at $t \sim 8000$ s. The saturation coverage of CO on Cu(997) is 0.52 ML, indicating that the $CO_2$ dissociation is not suppressed by coadsorbed CO. This may be due to the rapid diffusion of CO on the Cu surface as suggested by the STM experiments; the formed CO at an active site easily diffused to other adsorption sites even at $\sim 85$ K.

Fig. 4 shows the formation rates of CO estimated from the first derivative of the CO coverage change as a function of the reaction time displayed in Fig. 3(e). It clearly shows that the reaction rate increased gradually at low CO coverage. The result indicates that the clean Cu(997) is less reactive for $CO_2$ dissociation compared with Cu(997) with the adsorbates, and that the low reactivity of the clean surface leads to the induction period. Thus, $CO_2$ dissociation is facilitated by coadsorbed species. This may be consistent with previous theoretical calculations, which reveal that activation energy for the $CO_2$ dissociation on the clean Cu stepped surfaces is higher than 0.67 eV, indicating that the dissociation rarely occurs at 85 K.[15] The higher $CO_2$ pressure ($5.3 \times 10^{-6}$ Pa) leads to a faster increase in the reaction rate, followed by a decrease at
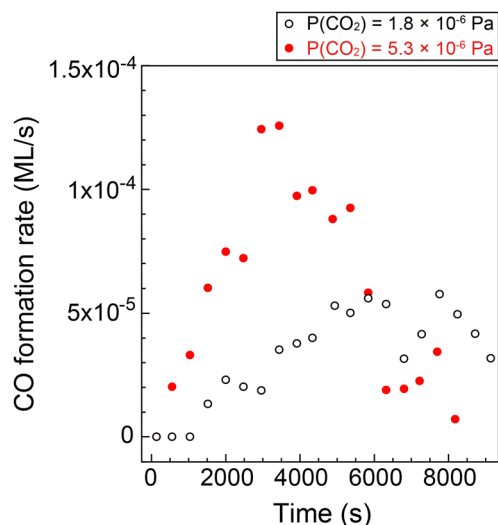
Fig. 4   CO formation rate on Cu(997) at 85 K as a function of the reaction time at $CO_2$ pressures of $1.8 \times 10^{-6}$ Pa (open black circles) and $5.3 \times 10^{-6}$ Pa (filled red circles). The rates were estimated from CO coverage shown in Fig. 4(e).

$t > 3500$ s. The gradual reduction of the reaction rate is probably due to the decrease of the active sites or hindrance of diffusion of the reaction product by adsorbed CO.

The small amount of oxygen atoms on the surface ($< 0.03$ ML) after the $CO_2$ dissociation suggests that the atomic oxygen produced was desorbed from the surface, probably *via* reaction with other molecules or atoms. Thus, we investigated the reaction products desorbed from the Cu(997) surface by QMS to reveal the details of the CO formation reaction from $CO_2$. The experimental setup is shown in Fig. 5(a). The Cu(997) surface at 82 K first faced the opposite direction to QMS. The isotopic $C^{18}O_2$ gas was introduced into the UHV chamber at a constant pressure ($1 \times 10^{-5}$ Pa). At 100 seconds after starting $CO_2$ flow into the chamber, the sample faced the QMS to detect reaction products desorbed from the surface. The QMS signals of selected masses are shown in the ESI† (Fig. S3). Note that reaction products were scarce compared with the feed gases, and it is difficult to distinguish the QMS signal of the product from those of background gases. Thus, the relative intensity of the QMS signals, *i.e.*, the intensity ratio of the QMS signal to the main $m/z = 48$ ($C^{18}O_2$) signal, is also shown in Fig. S3 (ESI†). The relative intensity of $m/z = 46$ ($C^{16}O^{18}O$) was increased when the sample faced the QMS ($t = 100$ s).

To validate that the increase of $m/z = 46$ relative intensity results from the surface reaction, a similar experiment was performed using a deactivated Cu(997) surface fully covered by multilayer cyclohexane (Fig. S4, ESI†). The relative intensities of $m/z = 46$ on both surfaces are shown in Fig. 5(b). The normalized $m/z = 46$ signal was steeply decreased at $t < 400$ s. This is due to the gradual increase of the $m/z = 48$ signal during this period (Fig. S4a, ESI†). The normalized signal was then increased at $t > 500$ s, possibly due to the reaction of $C^{18}O_2$ at the QMS ionization chamber or the ionization pressure gauge. Such behaviour was also observed in other possible
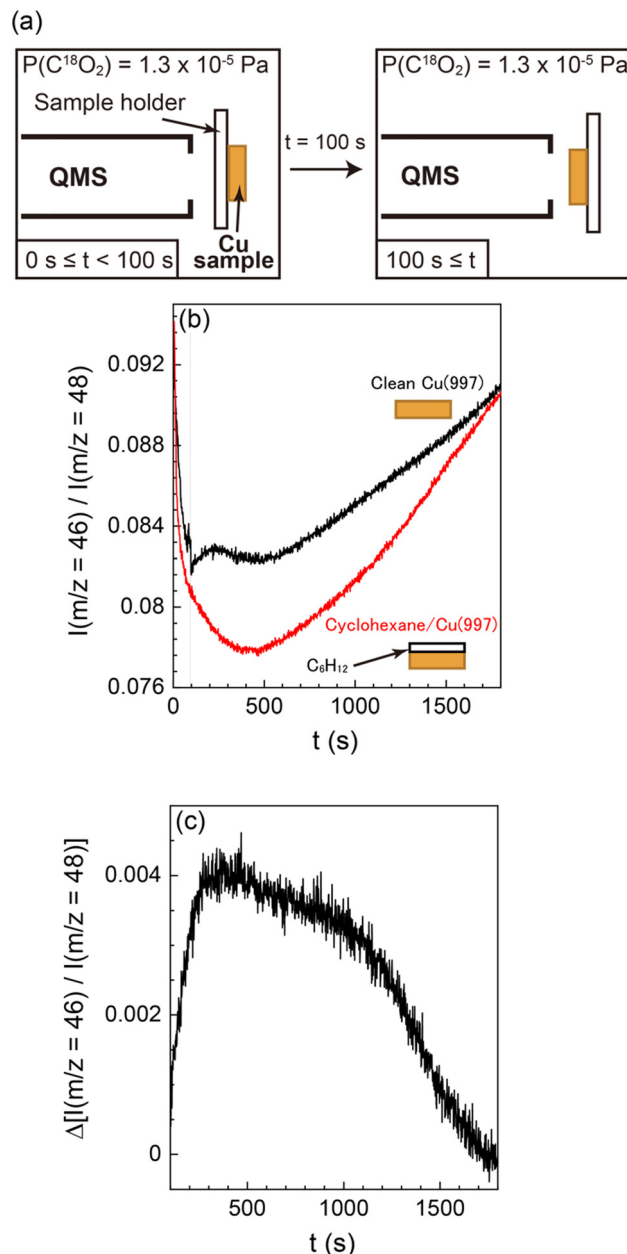


Fig. 5 (a) Experimental setup of QMS measurements of desorbed reaction products. First, the Cu(997) surface faced the opposite direction from QMS. At $t = 0$ s, $C^{18}O_2$ gas ($1 \times 10^{-5}$ Pa) was introduced in the UHV chamber, then facing the Cu(997) surface in the QMS direction at $t = 100$ s. (b) QMS signal ratio between $m/z = 46$ and 48 as a function of $CO_2$ exposure time using the bare Cu(997) (black) and the deactivated cyclohexane-covered Cu(997) (red) surfaces. (c) A differential of the QMS signals shown in (b). The surface temperature was maintained at 82 K.

reaction products ($m/z = 20$ ($H_2^{18}O$), 28 ($C^{16}O$), and 44 ($C^{16}O_2$) in Fig. S4b, ESI†). Thus, $C^{18}O_2$ molecules could be reacted with residual gases in the UHV chamber, such as $H_2$ and CO, probably at the hot filaments. However, the effect of such undesired reactions occurring at sites other than the Cu surface can be excluded by conducting the control experiment using the deactivated (cyclohexane-covered) surface under the same reaction condition.

**9230** | *Phys. Chem. Chem. Phys.*, 2024, **26**, 9226–9233

This journal is © the Owner Societies 2024

**Paper**

**PCCP**

There is a clear difference between the two surfaces; the increase in the relative intensity was observed on the "bare" Cu(997) surface, whereas there was no response in the signal when the cyclohexane-covered Cu(977) surface faced the QMS. This indicates that the increase in the relative intensity is due to the surface reaction on Cu(997). The signal difference of the two surfaces is shown in Fig. 5(c). The signal difference is monotonically increased up to $t \sim 400$ s, followed by a gradual decrease to zero at $t \sim 1700$ s. The observed time-dependent QMS signal of the desorbed $C^{16}O^{18}O$ shows a similar trend with the increase of the CO coverage by $CO_2$ dissociation in the SR-XPS experiments (Fig. 3). This suggests that the formation of $C^{16}O^{18}O$ is concomitant with the CO formation on the surface. The $C^{16}O^{18}O$ molecules are likely to be produced *via* oxidation of background $C^{16}O$ molecules in the UHV chamber. Therefore, a possible reaction mechanism of $CO_2$ in this experiment is an oxygen-exchange reaction with CO molecules on Cu(997): $C^{18}O_2$ (dosed gas) + $C^{16}O$ (background gas) $\rightarrow$ $C^{18}O$ (ad) + $C^{16}O^{18}O$ (gas). The oxygen-exchange reaction suggested by the QMS results is consistent with the SR-XPS results; only a small amount of atomic oxygen was detected on the Cu(997) surface during the reaction.

The $CO_2$ dissociation was also observed on the Cu(977) surface. The reactivity is similar to that of Cu(997), and the induction period was also observed on Cu(977) (see the ESI,† Fig. S5). Therefore, the $CO_2$ dissociation reaction is not sensitive to the structure of the Cu step facets. Fig. 6(a) shows O 1s XPS spectra of Cu(977) measured during $CO_2$ dissociation at $3 \times 10^{-6}$ Pa. The physisorbed $CO_2$ was first observed, followed by the growth of CO peaks at $\sim 533$ eV, which is similar to the Cu(997) surface. In addition, the effect of coadsorbed oxygen in the $CO_2$ dissociation was investigated. Prior to the $CO_2$ reaction, oxygen was dosed on the Cu(977) surface at 88 K. The O 1s spectrum of the oxygen-preadsorbed Cu(977) shows broad peaks between 528 eV and 532 eV. The oxygen coverage was estimated to be 0.06 ML from the peak intensity of the O 1s spectrum. After dosing $CO_2$ gas, the physisorbed $CO_2$ peak was first observed, and its intensity is slightly larger than those on the bare Cu(977) surface. Thus, preadsorbed oxygen creates more stable adsorption sites for $CO_2$. The gradual increase of $CO_2$ coverage in the SR-XPS experiment (Fig. 3) is probably due to the adsorption of a small amount of oxygen during the reaction. More importantly, the CO peak is clearly observed at $t = 1445$ s on the oxygen-preadsorbed Cu(977) surface, which is much faster that than on the clean Cu(977). This indicates that the coadsorbed oxygen promotes $CO_2$ dissociation. After the formation of CO, an O 1s peak was observed at $\sim 531$ eV, which can be assigned to atomic oxygen. The position of this peak is similar to that observed in the SR-XPS experiments (Fig. 3(b) and (d)). The chemical state of oxygen is changed from the initial O/Cu(977) surface by coadsorption with $CO_2$ or CO.

The observed promotional effect depends significantly on the coverage of preadsorbed oxygen. Fig. 7 shows the CO coverages as a function of the reaction time (88 K, $P_{CO_2} = 3 \times 10^{-6}$ Pa) at different preadsorbed-oxygen coverages. The results on the bare Cu(977) and O(0.06 ML)/Cu(977) surfaces show the
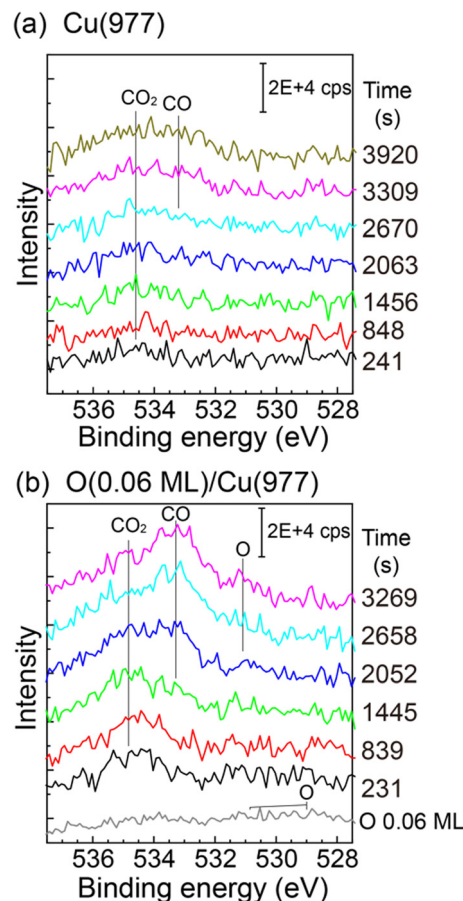


**Fig. 6** O 1s XPS spectra on (a) Cu(977) and (b) oxygen-preadsorbed Cu(977) at 88 K as a function of $CO_2$ exposure. $CO_2$ pressure was maintained at $3 \times 10^{-6}$ Pa during the measurements. The oxygen-preadsorbed Cu(977) was prepared before the $CO_2$ exposure by dissociative adsorption of $O_2$ at 88 K. The spectra were subtracted by the O 1s spectrum of clean Cu(977) to remove background Cu auger signals.
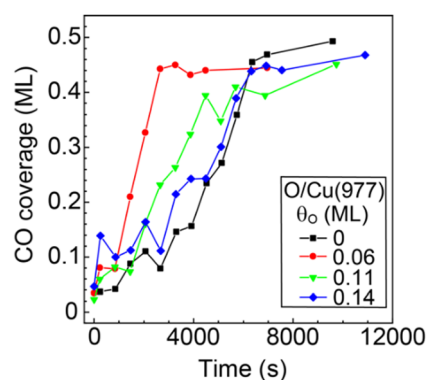


**Fig. 7** CO coverage produced from $CO_2$ dissociation on bare Cu(977) and oxygen-preadsorbed Cu(977) as a function of the reaction time. The sample temperature and $CO_2$ pressure were maintained at 88 K and $3 \times 10^{-6}$ Pa during the reaction.

significant shortening of the induction period by the existence of a small amount of oxygen. Preadsorption of further oxygen

This journal is © the Owner Societies 2024

*Phys. Chem. Chem. Phys.*, 2024, **26**, 9226–9233 | **9231**

($\theta_O$ = 0.11 and 0.14 ML) leads to a decrease in the reaction rates compared with that at $\theta_O$ = 0.06 ML. A small amount of oxygen required to promote the $CO_2$ dissociation suggests that the possible reaction site is an oxygen-adsorbed step or kink site, and that oxygen-adsorbed terrace sites suppress the dissociation reaction or diffusion of CO produced at the active sites to inactive vacant sites.

By a series of present experiments, the dissociation of the $CO_2$ molecules through the oxygen-exchange reaction with CO on the Cu(997) and Cu(977) surfaces was clearly observed. In addition, atomic oxygen adsorbed on the stepped Cu surface promoted the $CO_2$ dissociation at low temperatures (80–92 K). Recently, the activation of $CO_2$ molecules has also been studied under near-ambient pressure (NAP) conditions above room temperature. On the Cu(997) surface between 299 K and 340 K, the $CO_2$ dissociation and formation of CO, O, and $CO_3$ are observed at a $CO_2$ pressure of 80 Pa.[23,24] Kim *et al.* have revealed that the $CO_2$ dissociation into CO and O is also observed on Cu(997) at 300 K in the presence of 100 Pa $CO_2$.[25] In addition, high-pressure (HP) STM shows surface roughening and formation of partially oxidized Cu nanoclusters on the Cu(997) surface during the reaction.[25] Under a NAP condition, $CO_2$ is also dissociated into CO and O at step sites of the Cu(100) surface at 370 K in 40 Pa $CO_2$ gas.[26] An important point is that oxygen remains on Cu surfaces as atomic oxygen or $CO_3$ under the NAP conditions, whereas oxygen coverage on the Cu(997) surface was very low (less than 0.03 ML) under the UHV conditions investigated in this study.

The reaction mechanism of $CO_2$ on Cu surfaces observed under NAP conditions differed from those observed in this study under the UHV conditions. The observed difference between the UHV and the NAP experiments can be attributed to the difference in the activation energies of reactions. The previous theoretical study has shown that the activation energy for the $CO_2$ dissociation into CO and O on vicinal Cu surfaces is larger than 0.67 eV,[15] indicating that this reaction hardly occurs on clean Cu vicinal surfaces at low temperatures. Thus, the simple $CO_2$ dissociation reaction can occur only on the Cu surfaces above room temperature. However, based on the present experimental results, once such a rare dissociation event occurs at low temperature, atomic oxygen produced on the Cu surfaces can promote $CO_2$ dissociation. Note that the oxygen-exchange reaction could take place under both UHV and NAP conditions. Another possible reason for the different reaction pathways under NAP and UHV conditions might be the difference in the surface structures during the reactions; the HP-STM study shows the formation of Cu nanoclusters on the surface under the NAP conditions,[25] whereas the structural change of the Cu(997) was not observed at 80–92 K under the UHV conditions (Fig. 2). Therefore, the nature of active sites for the $CO_2$ dissociation can depend on the sample temperature that affects diffusivity of atoms and molecules and stability of reaction products on the Cu surfaces. Further theoretical studies on $CO_2$ dissociation at kink sites on Cu and the pre-adsorbed oxygen effect would be helpful in understanding the experimental results.

## Conclusions

The dissociation of $CO_2$ on the vicinal Cu surfaces at low temperatures was investigated using several experimental techniques. Dissociation of $CO_2$ molecules into CO on the Cu(997) and Cu(977) surfaces was observed at temperatures between 80 K and 90 K. In contrast, the reaction of $CO_2$ did not occur on the flat Cu(111), indicating that the defect sites, such as steps and kinks, play a key role in $CO_2$ dissociation. The XPS experiments show that CO and physisorbed $CO_2$ are the main adsorbates during the reaction. On the other hand, the amount of atomic oxygen on the surface was significantly smaller than that of CO. Analysis of desorbed reaction products during the reaction of isotopically labeled $CO_2$ revealed that the observed CO formation on the vicinal Cu surface is mainly due to the oxygen-exchange reaction with residual CO in a UHV chamber. The reaction of $CO_2$ on the vicinal Cu surface has an induction period; the initial reaction rate on the clean Cu surfaces was low, and the reactivity was gradually increased during the reaction. Once such a rare $CO_2$ dissociation event occurs at low temperature, atomic oxygen produced on the Cu surfaces may promote $CO_2$ dissociation.

## Conflicts of interest

There are no conflicts of interest to declare.

## Acknowledgements

## References

1 M. Aresta, *Carbon Dioxide as Chemical Feedstock*, WILEY-VCH Verlag GmbH and Co. KGaA, Weinheim, 2010.

2 W. Wang, S. Wang, X. Ma and J. Gong, *Chem. Soc. Rev.*, 2011, **40**, 3703–3727.

3 F. Solymosi, *J. Mol. Catal.*, 1991, **65**, 337–358.

4 H. J. Freund and M. W. Roberts, *Surf. Sci. Rep.*, 1996, **25**, 225–273.

5 U. Burghaus, *Catal. Today*, 2009, **148**, 212–220.

6 U. Burghaus, *Prog. Surf. Sci.*, 2014, **89**, 161–217.

7 J. Nakamura, Y. Choi and T. Fujitani, *Top. Catal.*, 2003, **22**, 277–285.

8 P. B. Rasmussen, P. A. Taylor and I. Chorkendorff, *Surf. Sci.*, 1992, **269**, 352–359.

9232 | *Phys. Chem. Chem. Phys.*, 2024, **26**, 9226–9233

This journal is © the Owner Societies 2024

9 J. A. Rodriguez, W. D. Clendening and C. T. Campbell, *J. Phys. Chem.*, 1989, **93**, 5238–5248.

10 P. A. Taylor, P. B. Rasmussen and I. Chorkendorff, *J. Vac. Sci. Technol., A*, 1992, **10**, 2570–2575.

11 K. H. Ernst, D. Schlatterbeck and K. Christmann, *Phys. Chem. Chem. Phys.*, 1999, **1**, 4105–4112.

12 I. A. Bönicke, W. Kirstein and F. Thieme, *Surf. Sci.*, 1994, **307**, 177–181.

13 S. S. Fu and G. A. Somorjai, *Surf. Sci.*, 1992, **262**, 68–76.

14 P. R. Davies and J. M. Keel, *Surf. Sci.*, 2000, **469**, 204–213.

15 F. Muttaqien, Y. Hamamoto, K. Inagaki and Y. Morikawa, *J. Chem. Phys.*, 2014, **141**, 034702.

16 T. Koitaya, S. Shimizu, K. Mukai, S. Yoshimoto and J. Yoshinobu, *J. Chem. Phys.*, 2012, **136**, 214705.

17 T. Koitaya, Y. Shiozawa, K. Mukai, S. Yoshimoto and J. Yoshinobu, *J. Chem. Phys.*, 2016, **144**, 054703.

18 P. Hollins and J. Pritchard, *Surf. Sci.*, 1979, **89**, 486–495.

19 B. E. Hayden, K. Kretzschmar and A. M. Bradshaw, *Surf. Sci.*, 1985, **155**, 553–566.

20 V. M. Browne, A. F. Carley, R. G. Copperthwaite, P. R. Davies, E. M. Moser and M. W. Roberts, *Appl. Surf. Sci.*, 1991, **47**, 375–379.

21 L. Bartels, G. Meyer and K. H. Rieder, *Appl. Phys. Lett.*, 1997, **71**, 213–215.

22 H. Tillborg, A. Nilsson and N. Martensson, *J. Electron Spectrosc. Relat. Phenom.*, 1993, **62**, 73–93.

23 T. Koitaya, S. Yamamoto, Y. Shiozawa, K. Takeuchi, R. Y. Liu, K. Mukai, S. Yoshimoto, K. Akikubo, I. Matsuda and J. Yoshinobu, *Top. Catal.*, 2016, **59**, 526–531.

24 T. Koitaya, S. Yamamoto, Y. Shiozawa, Y. Yoshikura, M. Hasegawa, J. Y. Tang, K. Takeuchi, K. Mukai, S. Yoshimoto, I. Matsuda and J. Yoshinobu, *ACS Catal.*, 2019, **9**, 4539–4550.

25 J. Kim, Y. Yu, T. W. Go, J. J. Gallet, F. Bournel, B. S. Mun and J. Y. Park, *Nat. Commun.*, 2023, **14**, 3273.

26 B. Hagman, A. Posada-Borbon, A. Schaefer, M. Shipilin, C. Zhang, L. R. Merte, A. Hellman, E. Lundgren, H. Gronbeck and J. Gustafson, *J. Am. Chem. Soc.*, 2018, **140**, 12974–12979.

This journal is © the Owner Societies 2024

*Phys. Chem. Chem. Phys.*, 2024, **26**, 9226–9233 | **9233**